

EXPERIMENTAL VERIFICATION OF KOZYREV'S INTERACTION OF NATURAL PROCESSES

© S.M. Korotaev, V.O. Serdyuk and M.O. Sorokin

Geoelectromagnetic Research Institute, Russian Academy of Sciences
(GEMRI P.O. Box 30, Troitsk, Moscow Region, 142092 Russia)

Abstract

A setup has been devised for measurement of effect of Kozyrev's interaction of the natural (geophysical and solar) processes, treated as macroscopic nonlocality. The detectors used in the setup had efficiency three orders of magnitude better than ones used before. Exhaustive steps had been taken to protect the detectors against noise-forming factors and to control them. As a result, effect of nonlocal influences of several large-scale processes related with the weather changes, the geomagnetic variations, the ionospheric and solar activity have reliable been detected. The large advanced lag has been found in a number of processes, that might be used in the geophysical forecasts.

1. Formulation of the problem

Properties of interaction of the dissipative processes discovered by N.A.Kozyrev [1] have been summarised in [2] (Sec.4, statements 1-5), and causal mechanical approach has been related with ideas of quantum nonlocality in the strong macroscopic limit and action-at-a-distance electrodynamics ([2], Sec. 5.1). From [2] operational consideration it is possible to formulate the following hypothesis:

$$\dot{S} = \sigma \int \frac{\dot{s}}{x^2} \delta\left(t^2 - \frac{x^2}{v^2}\right) dV, \quad (1)$$

where \dot{S} is the entropy production in the absorber (detector), \dot{s} is density of the entropy production in the sources, σ is cross-section of the interaction, x is distance, t is time, velocity v is bounded by $v^2 \leq c^2$, the integral takes over infinitely volume V . δ -function shows that interaction goes with a finite retardation and a symmetrical advancement.

Note, we expect that if interaction occurs through a medium with participation of the diffusion processes, reducing in any event on microlevel to electromagnetic interaction of the particles of a medium, then values of resulting retardation and advancement are large.

Straightforward estimations of the right side of Eq.(1) show that various and continuously occurring geophysical processes must give more effect in the detector than those which are simple to create in the lab. For the last power and minimal distance to the detector are essentially limited by creating by themselves noise-forming inflation, primarily by temperature one (as any enough sim-

ply realizable processes with great entropy change are accompanied, accordingly, by great thermal effect). That is why in this work influence upon the detector just the natural processes was studied.

2. Setting up an experimental problem

The task of the experiment is the detection of the entropy change of the environment according to Eq. (1) under condition of suppression of all known kinds of the classical local interactions. Although any dissipative process may be used as the detector, but one or other circumstantial connected with it observable is measured. Therefore choice of the detector type is resolved from the expected value of the relative effect. While all Kozyrev' s detectors have the efficiency about 10^{-5} , we had chosen by this criterion two types of the detectors with expected efficiency 10^{-2} - 10^{-1} . The first was based on measurements of the self-potentials of the weakly-polarised electrodes in the electrolyte, the second was based on measurements of the dark current of the photomultiplier. As the experiment implied, the first type turned out more appropriate, therefore consider its work in great detail.

Self-consistent solution for the potential u in the liquid phase is [3]:

$$u = \frac{2kT}{q} \ln \cos \left(x \arccos \exp \frac{q\zeta}{2kT} \right), \quad (2)$$

where q is charge of the main ion of the liquid phase, x is dimensionless length ($x=1$ corresponds to half of the distance between the electrodes), ζ is full (electrokinetic) potential. The entropy S can be expressed in term of the normalised potential ϕ :

$$\phi = \frac{u}{\int_0^l u dx}, \quad (3)$$

$$S = - \int_0^l \phi \ln \phi dx. \quad (4)$$

Substituting Eq. (2) to Eq. (3) and (4), after number of transformations one can obtain the expression for the entropy:

$$S \approx \ln 6 - 2 \ln(\arccos \exp w), \quad (5)$$

where

$$w = \frac{q\zeta}{2kT} < 0, \quad |w| \ll 1.$$

Taking into account that variations of ζ are small in comparison with the averaged value, we can linearize the time derivation of Eq.(5) and obtain the final simple expression for substituting to left side of Eq.(1):

$$\dot{S} \approx -\frac{I}{\sqrt{6}} \frac{|q|}{kT} \dot{\zeta}. \quad (6)$$

All known local factors influencing on ζ : temperature, pressure, chemism, illumination, electric field etc. must be excluded or stabilised. In fact, only difference $U = \zeta_1 - \zeta_2$ of pair of the electrodes can be measured. Except external screening, influence of mentioned noise-forming factors might be minimised by measuring U on minimal electrode space separation. In this case:

$$U = g(\zeta_1^c - \zeta_2^c), \quad (7)$$

where ζ^c are constants, g is efficiency of the detector, the measure of which is the variability coefficient.

For the detector based on the photomultiplier analogue of U is the work function. Noise-forming factors to be excluding or control are: temperature, electric and magnetic fields, illumination, moisture, feed voltage instability.

3. Setup and fulfilment of the experiment

The experimental setup included two types of the detectors and the apparatus for accompanying measurements.

The detector based on the weakly-polarised electrodes was constructed as follows. As the electrodes geophysical *C-Mn* ones were chosen. The electrodes were positioned in the glass vessel with the sub-saturated water solution of *NaCl*, space separation between the contact windows measured 1.5 cm. The vessel was rigidly encapsulated so that evaporation as well as atmospheric pressure variations were fully eliminated. The vessel was positioned in a dewar, covered on the outside by the additional layers of light and heat insulation. For remained temperature variations control the sensor of temperature (allowing to measure it continuously accurate to 0.001 *K*) was positioned between the internal wall of the dewar and the electrode vessel. Thus influence of all noise-forming factors, except temperature, was eliminated. Influence variation of the last was minimised and controlled. The quantity U was measured continuously accurate to 0.5 *mV*.

The second type detector was constructed on the base of the photomultiplier with *Cb-Cs* cathode of small area. The photomultiplier was positioned in the similar dewar with the temperature sensor and the additional external electric field screen. Possible magnetic field influence was controlled by the quantum modulus magnetometer accurate to 0.01 *nT*. The dark current I was measured continuously accurate to 0.05 *nA*.

Magnetic field measurement served also as indicator of the most important geophysical process – dissipation of the ionospheric electric current. Lastly, the overall air temperature in the lab was recorded continuously accurate to 0.1 *K*. Thus measurements on the setup included 2 major channels and 4 satellite ones.

As indicator of the synoptic processes we used continuous measurement of atmospheric temperature accurate to 0.1*K* at site remoted on 40 *km* off the setup kindly presented by A.N.

Morozov. The employment of remote reference data helps to exclude influence of the small-scale factors.

Accidentally absolutely independently, similar measurements of the electrodes self-potentials in other purposes were conducted by V.I. Nalivayko, kindly presented us his data. His setup did not provide measurements of the noise-forming and protection against them. Nonetheless, if a signal associated with the geophysical processes in U variations is sufficiently strong then, taking into account relatively small distance between the labs (300 m), it would have hoped on correlation of data. That is why V.I. Nalivayko's measurements were as 7-th channel in set of processing data.

The measurements carried out in continuous regime from 1996, December, 10 till 1997, December, 11.

Data were processed by the methods of causal, correlational, regressional and spectral analysis.

4. Results

4.1. Relation of the potentials on the remote setups

Above all it has a meaning to compare our measurements U with ones on the remoted (300 m) setup U_r . It immediately allows to establish, whether or not the variations of these quantities are merely the internal noises. The correlation coefficient turned out equal to 0.68 ± 0.01 . It is possible only one common trivial cause – the internal temperature. The partial correlation coefficient by eliminating influence of the internal temperature T_U of the detector U turned out equal to 0.74 ± 0.01 . Therefore local influence of the temperature is not a common cause of the correlated potential variations. It remains to consider such common cause nontrivial influence of the external geophysical processes.

4.2. Relation of the potentials with the internal, external and atmospheric temperature

Due to passive thermostating, dispersion of the internal temperature T_U of the air in the dewar of the detector U is very small (it is decreased on two orders relative to one of the external (lab) temperature T_e). Indeed, there is small correlation pike $r_{U|T_U} = -0.33 \pm 0.02$ (corresponding to the normal negative temperature coefficient of the electrodes $-141 \pm 9 \mu V/K$) which is accompanying by minima of the independence function [2] $i_{U|T_U} = 0.50_{-0.01}^{+0.02}$ and the causality function [2] $g = i_{U|T_U} / i_{T_U|U} = 0.97_{-0.01}^{+0.01}$ at the time shift $t = -20.4^h$ (negative sign of τ corresponds to retardation U relative to T_U). But at the positive time shift $\tau = 12.8^h$ there is great correlation pike $r_{U|T_U} = 0.87 \pm 0.01$ (anomaly positive sign) which is accompanying by minimum of $i_{U|T_U} = 0.43_{-0.00}^{+0.01}$ and maximum of $\gamma = 1.08_{-0.00}^{+0.01}$. Thus except normal causal relation $T_U \rightarrow U$, there is more strong anomaly unversed relation $U \rightarrow T_U$, therewith in both cases the effect is retarded relative to the

cause. For the short disturbances U their advancement relative to T_U one can note without any processing, directly in the records (Fig.1).

Turn now to analysis of connection U with the external (lab) temperature T_e . As there is no heat sources inside of the dewar, where T_U is measuring, then local connection of the potential variations with the temperature engages along the causal chain $T_e \rightarrow T_U \rightarrow U$. It imposes the restrictions on independences [4]:

$$i_{U|T_e} \geq \max(i_{T_U|T_e}, i_{U|T_U}), \quad i_{T_e|U} \geq \max(i_{T_e|T_U}, i_{T_U|U}). \quad (8)$$

Violation of Ineq. (8) (which are macroscopic analogue of Bell's inequations) is sufficient evidence of nonlocality of interaction T_e and U . It has turned out that $i(\tau)$ has 3 almost symmetrical minima at $\tau=0$ and $\pm 27.0^h$. It corresponds qualitatively to results of known Kozyrev's astrophysical experiment [4,5]. Asymmetry amounts to more strong connection of advanced interaction as compared to retarded one: at $\tau=-27.0^h$ $i_{U|T_e} = 0.81_{-0.00}^{+0.07}$, $i_{T_e|U} = 0.77_{-0.00}^{+0.10}$; at $\tau=0$ $i_{U|T_e} = 0.77_{-0.00}^{+0.10}$, $i_{T_e|U} = 0.72_{-0.00}^{+0.13}$; at $\tau=27.0^h$ $i_{U|T_e} = 0.75_{-0.00}^{+0.11}$, $i_{T_e|U} = 0.71_{-0.00}^{+0.12}$. Therewith independences of T_U and T_e have only single normal minimum: at $t = -11.5^h$ $i_{T_U|T_e} = 0.77_{-0.00}^{+0.03}$, $i_{T_e|T_U} = 0.84_{-0.00}^{+0.05}$, i.e. $T_e \rightarrow T_U$. Substituting these and mentioned above values of independences T_U and U , we concluded that there are two channels of connection T_e and U : classical local retarded and unusual nonlocal advanced. For the former at $\tau < 0$ left Ineq. (8) is asserted, for the last at $\tau > 0$ right Ineq. (8) is reliably violated.

Availability of the synchronous channel of connection. T_e with U is explained by interference of the retarded and advanced signals [7]. But symmetry by τ for T_e , U with asymmetry for T_U , U calls for analysis. If T_e and T_U both are connected with U by pairs of the symmetrical retarded and advanced channels, while T_e connected with T_U only by retarded one, it is easy to verify that $\delta^{\text{adv}} = \tau^{\text{adv}}(U|T_e) - \tau^{\text{adv}}(U|T_U) = \tau^{\text{adv}}(U|T_e) - [\tau^{\text{ret}}(U|T_U) - \tau^{\text{ret}}(T_U|T_e)]$. But $\tau^{\text{ret}}(T_U|T_e) = \tau^{\text{ret}}(U|T_e) - \tau^{\text{ret}}(U|T_U) = \delta\tau^{\text{ret}}$. Therefore $\delta^{\text{adv}} = 2\delta^{\text{ret}}$. Substituting mentioned above values τ , one can be content with $\delta^{\text{adv}} = 2\delta^{\text{ret}}$ accurate to 7%.

Consider now the variations of the atmospheric temperature T_a . Taking into account passive thermostating, the local causal connection $T_a \rightarrow T_e \rightarrow T_U$ must lead to weak correlation U with T_a at very long (many-days) retardation. In Fig.2 correlation of U and T_a is presented. Its most important feature is a dramatic exceeding of correlation at advancement U relatively T_a ($\tau > 0$) above retarded correlation ($\tau < 0$). Next there are five maxima $r_{U|T_a}$ at τ equal to -25, -13, 0, 13, 28 days. Symmetry relatively $\tau = 0$, notably for the main maximum 13^d is exactly analogous described above relation U with T_e . The greatest correlation is at $\tau = 13^d$: $r_{U|T_a} = 0.725 \pm 0.005$, The causal analysis has shown availability of corresponding minima of the independence function (at $\tau = 13^d$

$i_{UT_a}=0.72\pm 0.01$, $\gamma = i_{U|T_a} / i_{T_a|U} = 0.99_{-0.01}^{+0.00}$). Thus there is statistical reliable advanced connection of U with T_a .

The entropy of the environment roughly logarithmically related with the temperature. However it is very difficult to establish this relation quantitatively, taking into account the complicated weather processes (concerning also the solid Earth). In this sense the entropy production at the electromagnetic processes considered below is much conveniently.

4.3. Relation of the potentials with the geomagnetic variations

It is beyond reason to consider U depended on magnetic field F by any way. Therefore detection of relation of the potential with the geomagnetic variations would be a good test for the hypothesis (1), as these variations could be easy related with electric current dissipation in the source (ionosphere). Special experiments on influence on the detector of U by the artificial magnetic field (up to 100 A/m) in frequency range from 0 to 1 Hz had confirmed absence of any reaction of U within sensitivity of the apparatus.

Analysis shown existence of stable correlation $r_{UF} = -0.56\pm 0.01$ with great advancement U relative to F ($\tau=48.0^h$). In the causal analysis at this τ there is minimum $i_{F|U}=0.79_{-0.01}^{+0.02}$ ($\gamma=i_{U|F}/i_{F|U}=1.03_{-0.01}^{+0.01}$). Thus relation U and F is statistically reliable, but both from prior reasons and from advancement of U relative to F it can not be result of a direct influence of F on U . Therefore F is indicator of some process interacting with U .

Whereas the spectral amplitude ratio $U(f)/F(f)$ depends on frequency f , it has turned out that $U(f)/F^2(f)$ does not depend on f : $U(f)/F^2(f)=(1,7\pm 0,2)\cdot 10^{-5}\Omega m^2/A$. It is the most important result pointing to relation of U with the entropy production.

For proof consider application of Eq.(1) to the concrete case. The magnetic field F is related with the electric currents in the source – ionosphere, and also with the induced currents in the Earth. For simplicity of the problem, neglect by the last and consider the entropy production only in the source of F . It is easy to express the density of the entropy production through the electric field $E(f)$ (which in turn through the impedance $Z(f)$ is related with $F(f)$), the resistivity ρ and the medium temperature T . ρ and $Z(f)$ consider for simplicity as scalar. Then:

$$\dot{s} = \frac{\langle E^2(f) \rangle}{\rho k T} = \frac{|Z(f)|^2 \langle F^2(f) \rangle}{\rho k T}. \quad (9)$$

Combining Eq. (1), (6), (7) and (9) we obtain:

$$U(f) = \frac{\sqrt{6}}{4\pi} \frac{T_u g \sigma}{|q| f} \int \frac{|Z(f)|^2 F^2(f)}{\rho T x^2} dV. \quad (10)$$

Eq. (10) can be simplified using the known properties of electromagnetic field of the ionospheric source [9]. First, the field F is well approximated by the plane wave, therefore it is possible

to factor out the F^2 from the integral. Second, using quasi-steady-state approximation of the plane wave impedance, substitute $|Z(f)|^2 = 2\pi f\mu_0\rho$ in Eq.(10). As a result we have:

$$\frac{U(f)}{F^2(f)} = \frac{\sqrt{6}}{2} \frac{T_U g \sigma \mu_0}{|q|} \int \frac{dV}{Tx^2} = \text{const.} \quad (11)$$

Thus the experimental fact $U(f)/F^2(f)=\text{const}$ is explained within the Eq. (1).

It is of interest to estimate the constant σ from observations. If presented reasoning with references to Kozyrev`s concept has meaning, the value σ could be related with known Kozyrev`s constant of course of time c_2 (velocity of causal-effect transition on the microscopic level). From theoretical consideration $c_2 \rightarrow \infty$ in the classical limit, while from the causal-mechanical experiments $c_2=(2,2\pm 0,1)10^6$ m/s [1]. As on this stage only order of σ is of interest, for its estimation simplify Eq.(11), supposing, that similarly to an ordinary electromagnetic field, it is possible to employ the plane wave approximation. Then, instead of Eq.(11), we have

$$\frac{U(f)}{F^2(f)} = \frac{\sqrt{6}}{2} \frac{T_U g \sigma \mu_0 h}{|q|T}, \quad (12)$$

where h is thickness of the dynamo-layer. For estimation of s accept corresponding to the detector parameters: $T_U=3\cdot 10^2 K$, $q=1.6\cdot 10^9 A\cdot s$, $g=6\cdot 10^2$, and known (e.g. [10]) typical values of the ionospheric parameters: $\dot{O}=10^3 \hat{E}$, $h=5\cdot 10^4 m$. Then with mentioned above value $U(f)/F^2(f)$ we obtain from Eq.(12) $\sigma=2\cdot 10^{-21} i^2$. It is most reasonable value – of order an atom cross-section. And really this value may be related with c_2 , mass and charge of an electron:

$$\sqrt{\sigma} \approx \frac{e^2}{m_e c_2^2}. \quad (13)$$

If Eq.(13) is true, then in the classical limit $\sigma \rightarrow 0$.

4.4. Relation of the potentials with the ionospheric activity

It has been turned out that probability of the sudden ionospheric disturbances during phase of increasing U far exceeds this probability during phase of decreasing. Probabilities ratio is 4.5. If only sudden enhancements of atmospherics were selected such probability ratio became to 7.1.

It may be suggested following qualitative interpretation of these facts. Sudden ionospheric disturbances are sharp increasing of ionization of the lower ionosphere. That corresponds to decreasing of the entropy resulting, according Eq.(1) and (6), to increasing potentials. In the case of sudden enhancements of atmospherics there is an additional effect related with enhancements of the thunderstorm activity.

6.4. Relation of the potentials with the solar activity

The spectral analysis has shown similarity of the spectra U and solar activity indices. In particular, there is a maximum at the period 27^d with amplitude about millivolt.

The analysis in time domain gives more detailed information. So far as time averaged solar-terrestrial data always demonstrate stronger dependence, we processed our data with daily and monthly averaging. The former were processed by the causal and correlation analysis, the last - only by correlation one (because the causal analysis needed larger statistics).

Consider daily averaged data. In Fig.2 the synchronous independence function U on the solar radio wave flux R (in the standard range 245... 15400 MHz) and their correlation function are shown. Both curves point out the optimal frequency 1415 MHz , corresponding the radiation from the level of the lower corona-upper chromosphere, where the most intensive dissipative processes take place. At this frequency $i_{UR} = 0.66_{-0.00}^{+0.02}$ ($\gamma = i_{UR} / i_{R|U} = 0.81 \pm 0.01$), $r_{UR} = 0.68 \pm 0.02$. All these serieses R were taken reduced to 1A.U. It can expect that use an observable series R instead of reduced one has to increase correlation slightly. Indeed at the frequency 2800 MHz for which both serieses of R are presented in the "Solar-Geophysical Data", it turns out that for reduced $r_{UR} = 0.59 \pm 0.02$, while for observable R : $r_{UR} = 0.62 \pm 0.02$.

One can suggest the cosmic ray flux as a possible local mechanism of influence of the solar activity on the detector. We have tested it by data of the IZMIRAN neutron monitor, situated near (100m) our setup. Correlation of U with the cosmic ray counting rates turned out much less of above and below mentioned correlation U with R : -0.30 ± 0.03 at daily averaging and not significant at monthly averaging. Therefore cosmic rays are not carriers of the interaction.

Maximum of dependence U on R (corresponding to min $i_{U|R}$) is at large advancement U relative to R . For the optimal frequency 1415 MHz min $i_{UR} = 0.59_{-0.00}^{+0.01}$ (and min $\gamma = 0.71 \pm 0.01$) is at $\tau = 39^d$. The ratio of i_{UR} at advancement $\tau = 39^d$ and symmetrical retardment $\tau = -39^d$ turned out inverted to the ratio of corresponding r_{UR} : $i_{U|R}^{ret} / i_{U|R}^{adv} = r_{UR}^{adv} / r_{UR}^{ret} = 1.3$.

Monthly averaged data have demonstrated this advanced connection even more brightly. In Fig.3 such data of U and R shifted on 1 month are presented. The strong correlation is obvious. At $\tau = 1^M$ $r_{UR} = 0.76 \pm 0.08$. At symmetrical $\tau = -1^M$ correlation is not significant.

Thus we have to consider influence of the solar activity on the U as direct (nonlocal) with advanced lag of about a month.

4.6. Results with the dark current detector

All mentioned above effects (except of the sudden ionospheric disturbances) were discovered also with the detector of dark current I , but they were rather week as compared with U . As this takes place the strong interplay of I and U , not reducing to trivial influence of the single common local cause, which is the lab temperature T_e has been uncovered. It might be demonstrated by Fig.5. It is seen good similarity of spectra I and U (in particular, exact fit of the amplitude maxima at the periods 28.2^h and 16.6^h). On the contrary the spectrum T_e appears quite different. E.g. the period of the main low frequency maximum T_e 60h is respectively 1.2 and 2.0 times shorter than of the main maxima I and U .

In Fig.6 the functions $i_{U|I}$, $i_{I|U}$ and $\gamma=i_{U|I}/i_{I|U}$ are shown, positive value τ corresponds to retardation I relatively U . At $\tau = -11.5^h$ and $\tau = 15.5^h$ two deep minima of independences are seen: $i_{I|U}(\tau^{ret}) = 0.57_{-0.00}^{+0.02}$, $i_{U|I}(\tau^{adv}) = 0.47_{-0.01}^{+0.02}$. These minima correspond to maxima $\gamma = 1.20_{-0.01}^{+0.01}$ (and maxima of correlation: 0.73 ± 0.01 and 0.76 ± 0.01 respectively).

We have to infer that U and I are connected nonlocally, in so doing T_e acts as a classical channel of communication (in spite of weakness of connection through T_e). Just exceeding dependence of observables over expected by a local channel is the characteristic feature of nonlocality. Nonlocality in light of Wheeler-Feynman theory is compatible with availability of true advanced interaction [7] (in terms of the causal analysis $\gamma > 1$ as at $\tau > 0$ so at $\tau < 0$). If the hypothesis is right, asymmetry of the extrema relatively $\tau = 0$ in Fig.6 can be explained. The dewars of both detectors are the same, but unlike the electrode detector (Sec. 4.2), in the dark current detector local influence of the internal temperature T_I on I occurs for small time $\tau \approx 0$ (accurate to 1^m) therefore $\tau^{ret}(T_U/T_e) = \tau^{ret}(T_I/T_e) = \tau^{ret}(I/T_e)$. Influence U on I proceeds in positive time through T_e and in negative time by the direct channel. Here from, by reference to the same values of τ to those in Sec. 4.2, we obtain: $\tau^{ret}(I/U) + \tau^{adv}(U/I) = \tau^{ret}(U/T_U) + \delta^{ret} = 27^h$, $\tau^{adv}(U/I) = \delta^{ret} = 11.5^h$, and hence $\tau^{ret}(I/U) = 15.5^h$ - which are in exact accord with the results presented in Fig.6.

A peculiarity of I as an indicator of the natural dissipative processes is that sometimes the standard deviation of I displays more spectacular relationship with them than the averaged I . In Fig. 7 amplitude spectra of the solar radio wave flux R and the standard deviation of I are shown. The left amplitude pike has the period 27^d .

5. Conclusion

Results of the long-term experiment performed on the modern level of rigour allow to make positive inference on the existence of Kozyrev' s interaction of the dissipative processes. This interaction is essentially nonlocal. Although we are far to respect to Eq.(1) more seriously as to heuristic one, this simplest formulation has turned out having experimentally verified predictability. Therefore as theoretical so experimental further studies of Kozyrev' s interaction, the studies concerning macroscopic nonlocality, causality and nature of time are of profound interest.

Acknowledgements

This work was supported by RFBR (grant №96-05-64029). The authors thanks J.M. Abramov for participation in the experiment.

References

1. *N.A. Kozyrev*, «Selected Works». LSU-Press, Leningrad (1991) (in Russian). The main results concerning the topic had been published in English: *N.A. Kozyrev*, «On the possibility of experimental investigation of properties of time». In: Time in science and philosophy, Academia, Prague, P. 111-132. (1971).
2. *S.M. Korotaev*, Force of time. In this edition.
3. *S.M. Korotaev*, Filtration electromagnetic field of the submarine springs. Izvestia Phys. of the Solid Earth. №8. P.91-95. (1979).
4. *S.M. Korotaev, S.V. Shabelyansky and V.O. Serdyuk*, Generalized causal analysis and its employment for study of electromagnetic field in the ocean. Izvestia Phys. of the Solid Earth, 16. P.77-86. (1992).
5. *N.A. Kozyrev and V.V. Nasonov*, New method of determination of trigonometric parallaxes on the base of difference between actual and visible position of the stars. In: Astrometry and Heavenly Mechanics. VAGO Press, Moscow-Leningrad, P.168-179. (1978) (In Russian).
6. *N.A. Kozyrev and V.V. Nasonov*, On some properties of time detected by astronomical observations. In: Manifestation of Cosmic Factors on the Earth and Stars. VAGO Press, Moscow-Leningrad, P.76-84. (1980).
7. *J.C. Cramer*, Generalized absorber theory and the Einstein-Podolsky-Rosen paradox. Phys. Rev. D. **Vol.22**. 12. P.362-376. (1980).
8. *P.P. Chambadal*, Evolution et Applications du Concept D' Entropie. Dunod, Paris. (1963).
9. *I.I. Rokityansky*, Geoelectromagnetic Investigation of the Earth's Crust and Mantle. Springer-Verlag, Berlin (1982).
10. Illustrated Glossary for Solar and Solar-Terrestrial Physics. Ed. by A. Bruzek and C.J. Durrant. D.Reidel Publ.Co., Dordrecht (1977).

Figure captions

- Fig.1. An example of synchronous records of the potentials U and T_U , t is time in hours.
- Fig.2. Correlation function U and atmospheric temperature T_a r_{UTa} . τ is time shift of T_a relation to U in days.
- Fig.3. Independence of U on solar radio wave flux R $i_{U/R}$ and their correlation r_{UR} as functions of frequency f of R .
- Fig.4. Monthly averaged year serieses of U and R (at $f=1415$ MHz). Time axis of R t_R^M is shifted to one of t_U^M on $\tau^{\text{adv}}=1$ month.
- Fig.5. Amplitude spectra of the dark current I , U and the external (lab) temperature T_e in period range from 5 hours to 10 days. t is period in hours, f is frequency in microherz.
- Fig.6. Independence functions of U and I i and causality function γ . τ is time shift I relative to U in hours.
- Fig.7. Amplitude spectra of solar radio wave flux R (at $f=610$ MHz) and daily standard deviation of the dark current $\sigma(I)$ in period range from 24 days to half of year. t is period in days, f is frequency in microhertz.

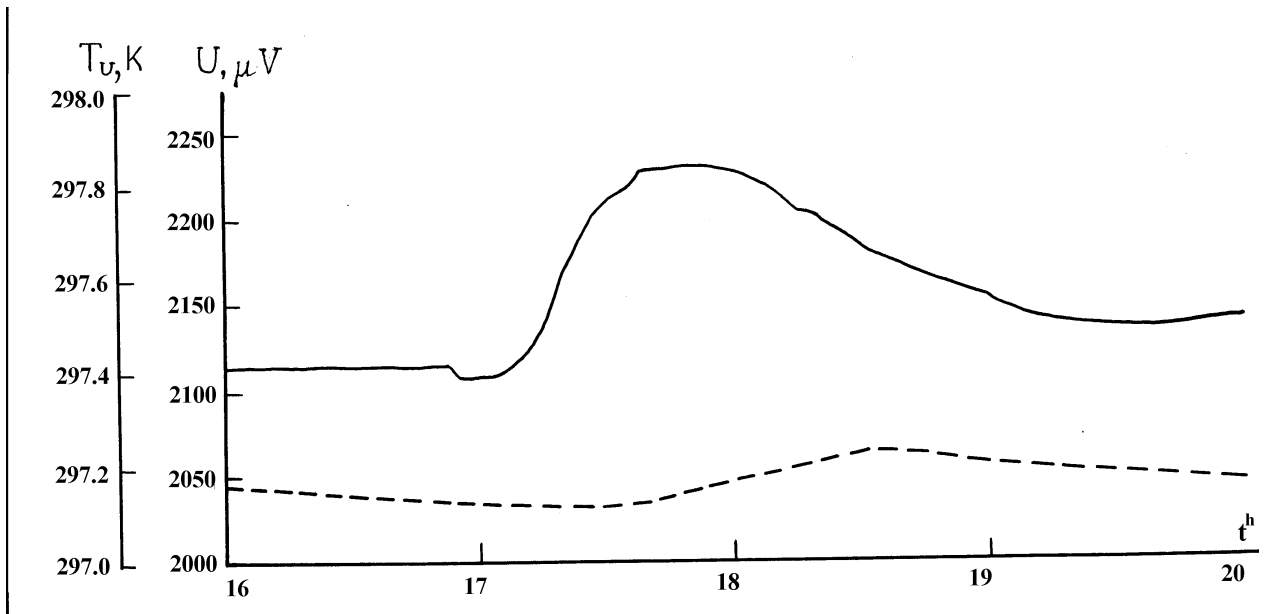


Fig. 1

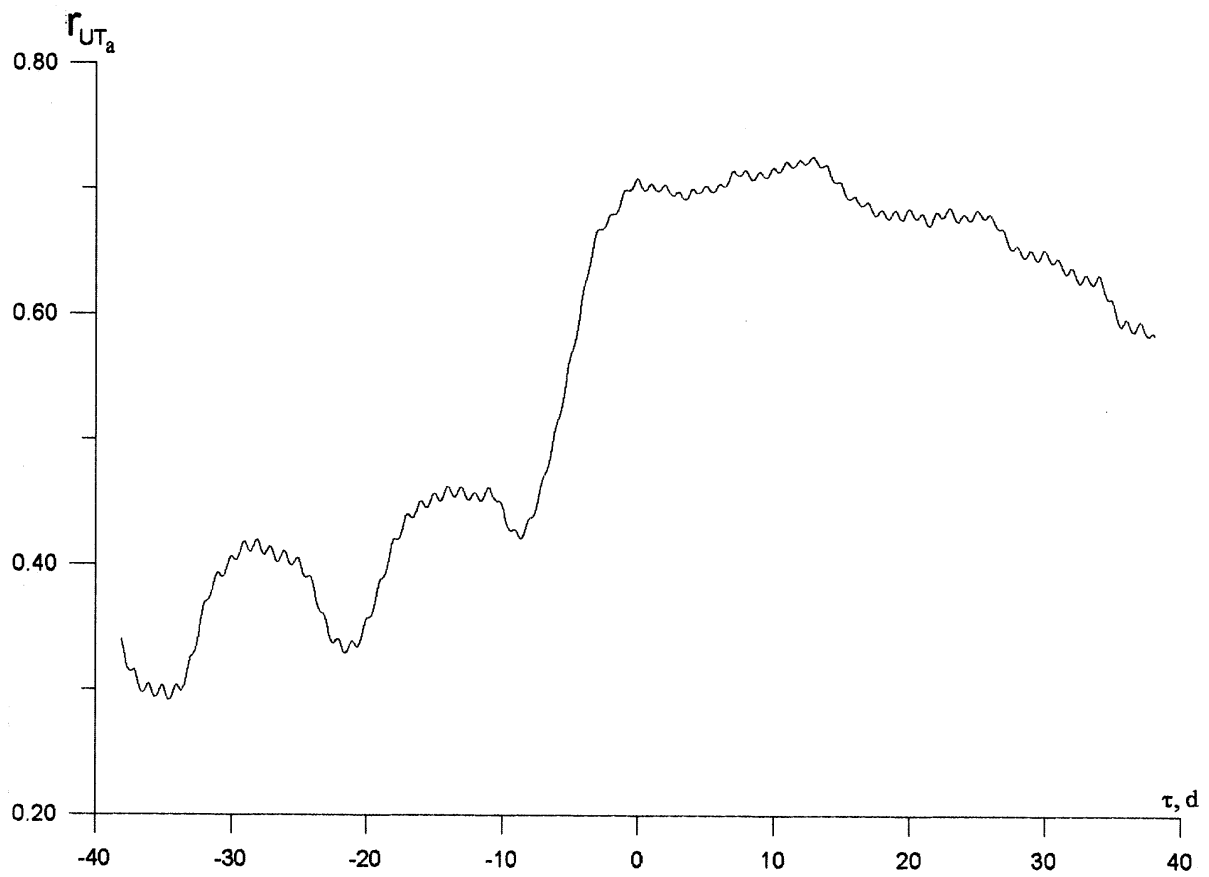


Fig. 2

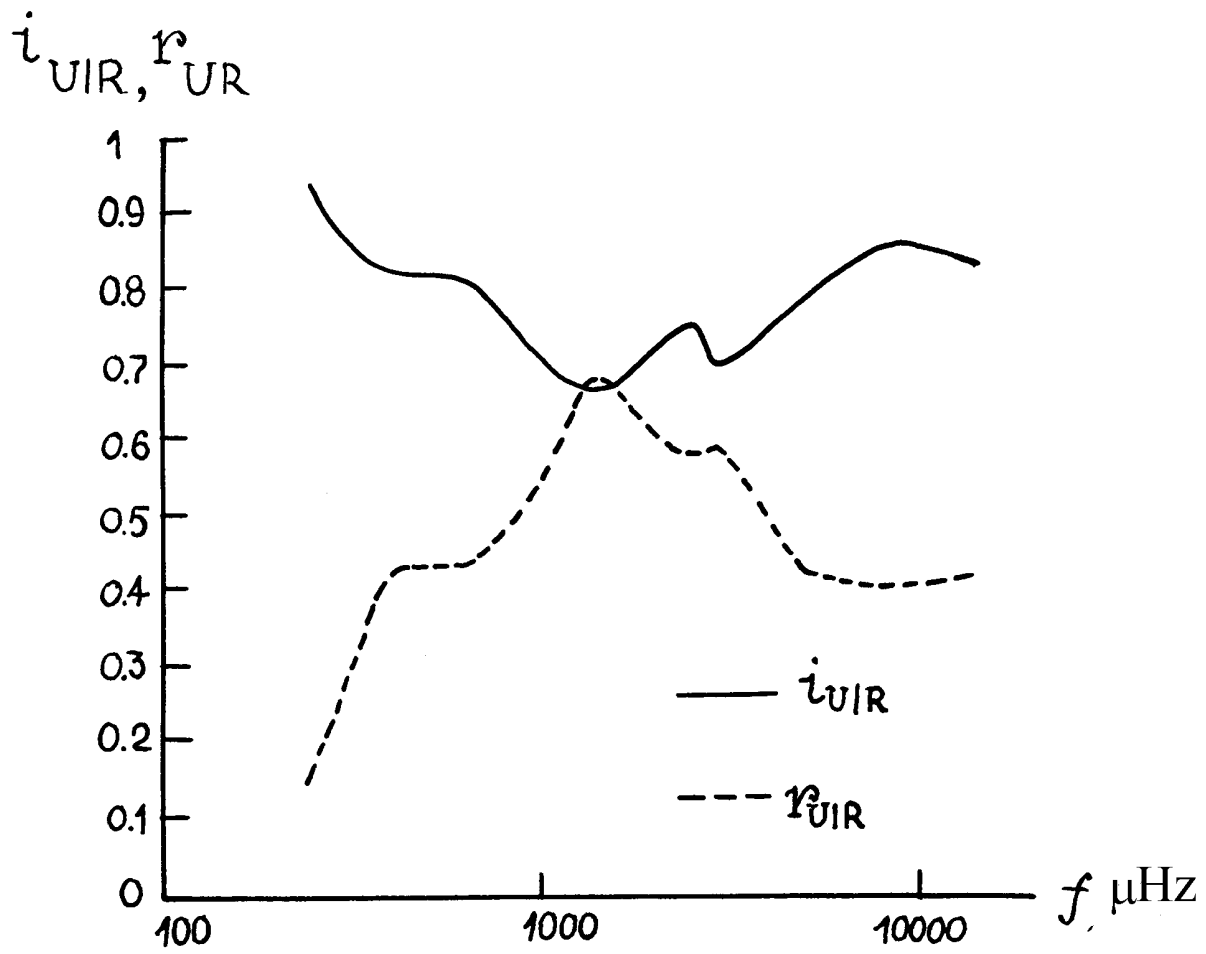


Fig. 3

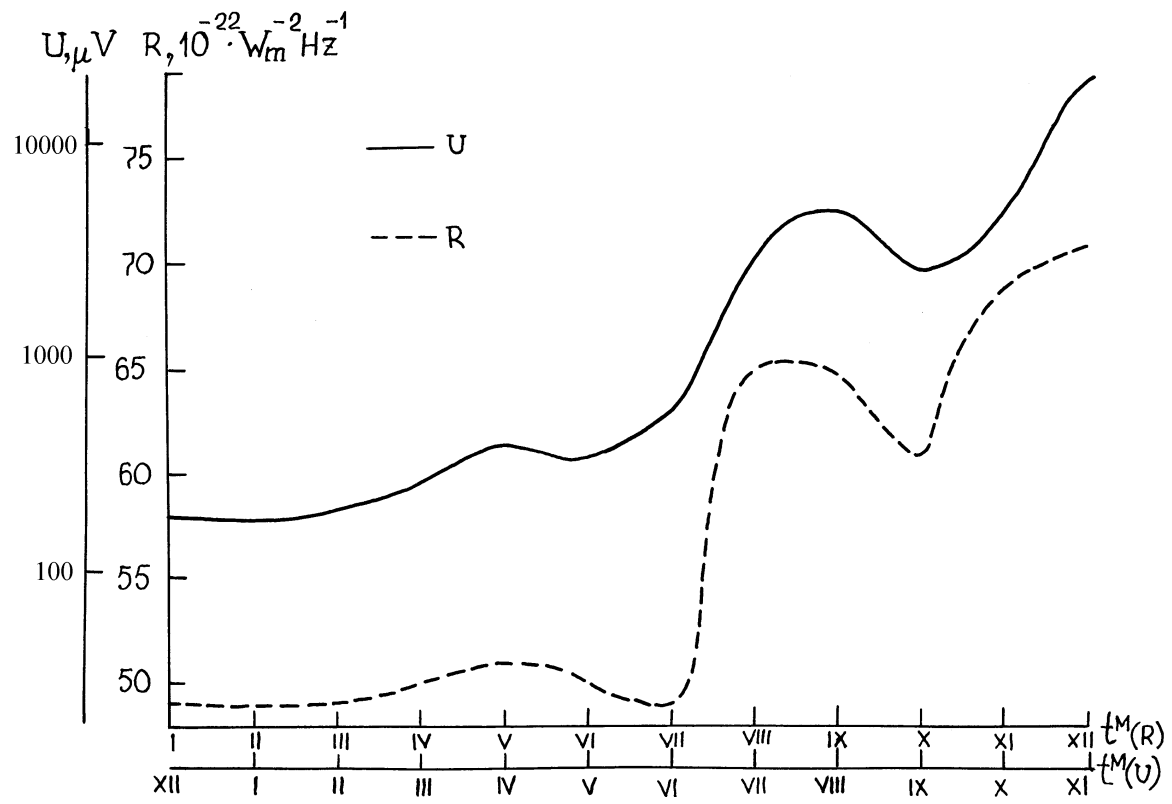


Fig. 4

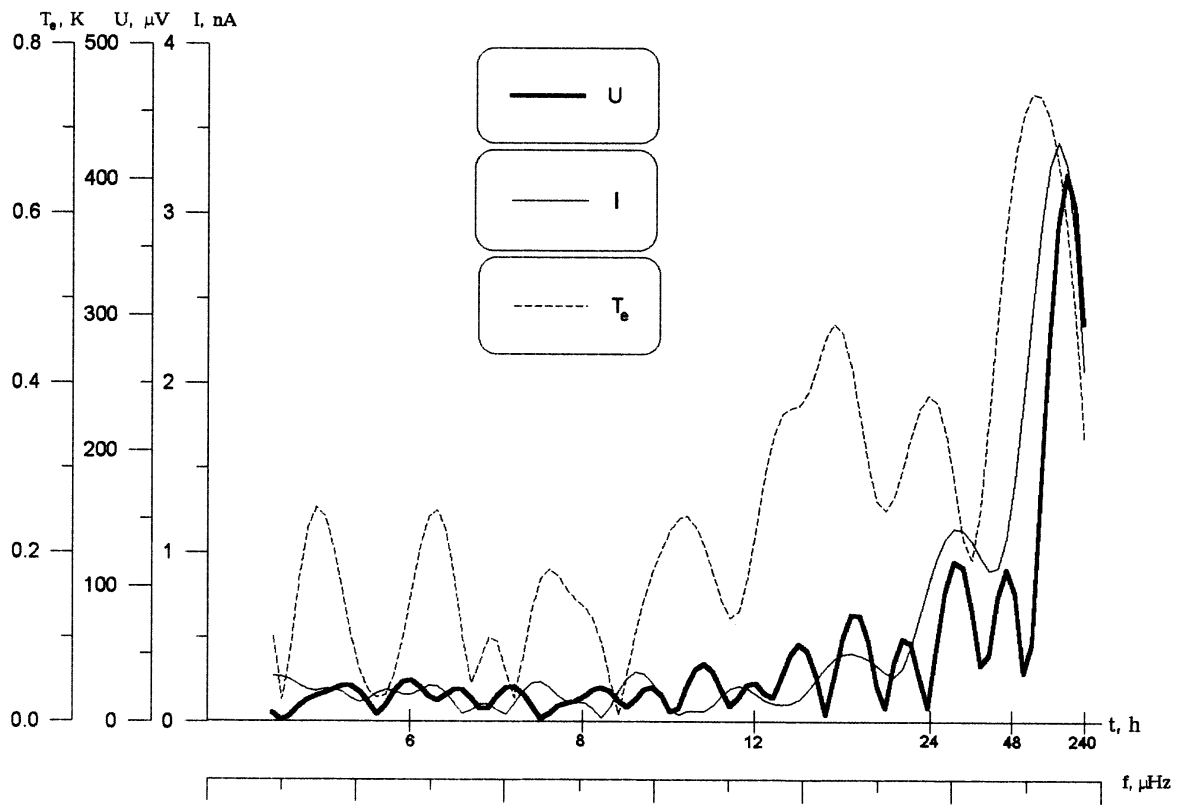


Fig. 5

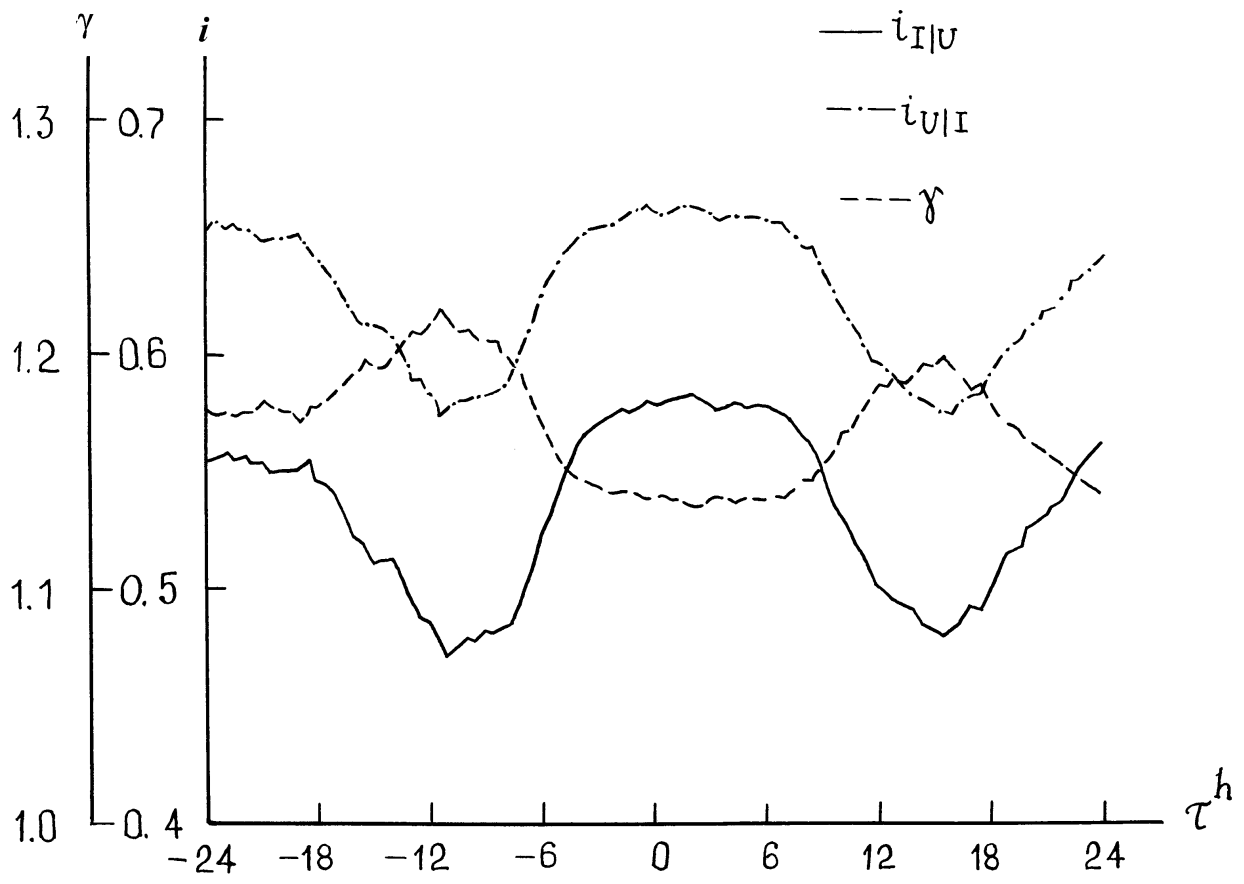


Fig. 6

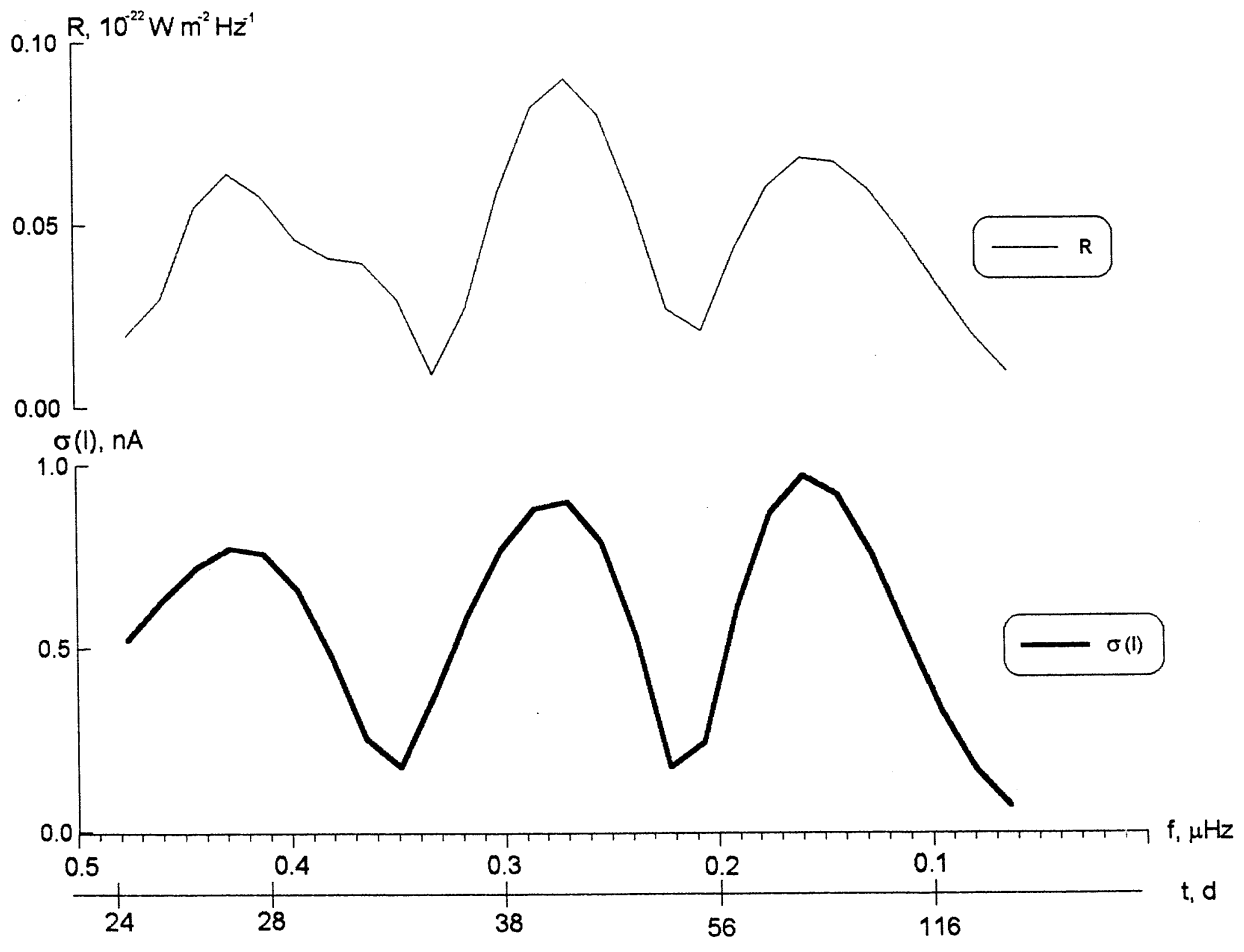


Fig. 7